nary criteria.[6-8] However, the values observed in the other studies are not the same as those in the present study because we analyzed the interpretation both visually and statistically. Recent studies have shown that the diagnostic capability of visual analysis of ^{18}F-FDG-PET increases when the raters interpret the images in combination with 3D stereotactic surface projections.[14,15] These kinds of visual-statistical methods seem to be a standard approach in clinical settings.

To increase the concordance rate and diagnostic capability, we need to overcome some problems. We had to degrade the image quality according to the PET with the lowest quality among the 23 facilities of J-ADNI.[11] Therefore, the quality of the images may be improved in the future. In addition to the image quality, development of new methods or new approaches to image interpretation may contribute to increasing the concordance.

This study showed a relationship between combined visual-statistical interpretation and automated quantitative assessment regarding the characteristic AD pattern in brain ^{18}F-FDG-PET. Significant association was observed between the quantitative index (FDG-PET score) and the number of raters who interpreted the scans accordingly. This correlation may have been something expected from reports on similar/automated analysis.[5,6] However, this association was observed in a large-scale multicenter study by using various camera models on a wide spectrum of subjects in the present study.

From the standpoint of detecting the AD pattern, cases evaluated as having positive AD findings by complete agreement of all 3 raters tended to show a higher quantitative index than the cases that fewer than 3 raters interpreted as having positive AD findings. From the standpoint of ruling out the AD pattern, cases evaluated as having negative AD findings by complete agreement of all 3 raters also tended to show a lower quantitative index than the cases that fewer than 3 raters interpreted as having negative AD findings. Therefore, the results suggest that interpretation by 3 raters may be better than that by 2 or fewer raters. The results also indicate that cases that only 1 rater interpreted as having positive (or negative) AD findings presented a different quantitative index from those that no raters interpreted as having positive (or negative) findings. This outcome suggests that there are cases in which the "minority opinion" may not be ignored.

Generally, the minority opinion is somewhat important when a subtle but definite finding is evaluated. However, most of the ^{18}F-FDG-PET images for which the judgment did not agree among the raters showed ambiguous findings. Ng et al[6] reported that experienced raters scored higher accuracy than nonexperienced raters in the interpretation of brain ^{18}F-FDG-PET images for the diagnosis of AD.[6] Such subtle findings in brain ^{18}F-FDG-PET may be difficult to interpret. We need to analyze the difference in detail and develop new methods for interpretation or new diagnostic tools.

When the FDG-PET score of the cases judged as P1 in the consensus read were examined, NC subjects with P1 interpretation showed lower FDG-PET scores than MCI and AD subjects. This result is probably because many of the NC subjects with P1 interpretation presented with a very mild AD pattern that influenced the FDG-PET score to only a small extent. Those cases, however, presented characteristic findings such as posterior cingulate hypometabolism, which led to the P1 interpretation.

The criterion standard used in this study was the clinical diagnosis at enrollment. Although dementia with Lewy body cases with the specific symptoms were excluded from enrollment in the J-ADNI beforehand, differentiating Lewy body dementia from AD is occasionally difficult in clinical settings.[16] The typical Lewy body dementia pattern of ^{18}F-FDG-PET, evaluated as occipital hypometabolism, is classified into P1+ by the criteria of Silverman et al.[1] Some cases classified into P1+, though limited in the present study, seem to have the possibility of Lewy body dementia. Moreover, the consensus read judged 16 of 107 cases of the NC group to be the AD pattern (P1 and P1+), and 8 of 67 cases in the AD group to be a non-AD pattern (N1 and P2). These disagreements might be either caused by inappropriate clinical diagnosis at enrollment or reflecting the limitation of FDG-PET as a diagnostic tool. While these diagnostic discrepancies are not critical in the present study, which analyzed inter-rater concordance, comparison with other criterion standards such as long-term follow-up or postmortem examination is important for this kind of multicenter study in the future.

The FDG-PET score of 1.0, by definition, is proposed as an optimum threshold for the differential diagnosis of AD from healthy subjects.[5] Because the present study deals with comparison of combined visual-statistical human interpretation with automated quantitative analysis, we derived a cutoff level of 0.67 based on discrimination of the P1 from the N1 pattern. This discrepancy may be explained by the difference in the target of discrimination as well as in the profile of subjects, and the lower cutoff would be consistent with a higher sensitivity for visually detecting the AD pattern than for clinically identifying the diagnosis of AD, for which the 1.0 cutoff is designed. In addition, one of the essential factors for this discrepancy seems to be that decisions by visual-statistical interpretation are not completely consistent with the actual clinical diagnosis. Because the diagnostic capability of ^{18}F-FDG-PET is not the subject of the present study, further studies are needed to elucidate the discrepancy.

CONCLUSIONS

Inter-rater agreement was moderate to substantial regarding the combined visual-statistical human interpretation of the characteristic AD pattern in ^{18}F-FDG-PET. In addition, a significant relationship between human interpretation and automated quantitative assessment was found. The human rating as an AD or normal pattern was best predicted by the FDG-PET score when using a cutoff of 0.67.

ACKNOWLEDGMENTS

The authors thank the J-ADNI Imaging Pharmaceutical Industry Scientific Advisory Board and other organizations for their support of this work.

Disclosures: Tomohiko Yamane—*RELATED: Grant*: New Energy and Industrial Technology Development Organization of Japan,* *Comments*: This study is a part of the "Translational Research Promotion Project/Research Project for the Development of a Systematic Method for the Assessment of Alzheimer's Disease," sponsored by the New Energy and Industrial Technology Development Organization of Japan. The Japanese Alzheimer's Disease Neuroimaging Initiative is also supported by a Grant-in-Aid for Comprehensive Research on Dementia from the Japanese Ministry of

Health, Labour and Welfare, as well as by grants from J-ADNI Pharmaceutical Industry Scientific Advisory Board companies. Yasuhiko Ikari—*UNRELATED: Employment*: Micron. Tomoyuki Nishio—*UNRELATED: Employment*: Micron. Takashi Kato—*RELATED: Grant*: government-based funding, *Comments*: Ministry of Health, Labour, and Welfare in Japan; Ministry of Education, Culture, Sports, Science & Technology in Japan. Kengo Ito—*RELATED: Grant*: "Translational Research Promotion Project/Research Project for the Development of a Systematic Method for the Assessment of Alzheimer's Disease," sponsored by the New Energy and Industrial Technology Development Organization of Japan, and a Grant-in-Aid for Comprehensive Research on Dementia from the Japanese Ministry of Health, and Labour and Welfare.* Michio Senda—*RELATED: Grant*: Research Association for Biotechnology,* *UNRELATED: Grants/Grants Pending*: GE Healthcare,* Eli Lilly.* Morihiro Sugishita—*RELATED: Grant*: New Energy and Industrial Technology Development Organization,* *Support for Travel to Meetings for the Study or Other Purposes*: New Energy and Industrial Technology Development Organization, *UNRELATED: Consultancy*: Eli Lilly Japan KK, *Employment*: Sugishita Co Ltd, *Royalties*: Nihon Bunka Kagakusha Co Ltd, *Stock/Stock Options*: Japan Air Line. *Money paid to the institution.

REFERENCES

1. Silverman DH, Small GW, Chang CY, et al. **Positron emission tomography in evaluation of dementia: regional brain metabolism and long-term outcome.** *JAMA* 2001;286:2120–27
2. Mosconi L, Perani D, Sorbi S, et al. **MCI conversion to dementia and the APOE genotype: a prediction study with FDG-PET.** *Neurology* 2004;63:2332–40
3. Yuan Y, Gu ZX, Wei WS. **Fluorodeoxyglucose-positron-emission tomography, single-photon emission tomography, and structural MR imaging for prediction of rapid conversion to Alzheimer disease in patients with mild cognitive impairment: a meta-analysis.** *AJNR Am J Neuroradiol* 2009;30:404–10
4. Herholz K, Salmon E, Perani D, et al. **Discrimination between Alzheimer dementia and controls by automated analysis of multicenter FDG-PET.** *Neuroimage* 2002;17:302–16
5. Herholz K, Westwood S, Haense C, et al. **Evaluation of a calibrated ^{18}F-FDG-PET score as a biomarker for progression in Alzheimer disease and mild cognitive impairment.** *J Nucl Med* 2011;52:1218–26
6. Ng S, Villemagne VL, Berlangieri S, et al. **Visual assessment versus quantitative assessment of ^{11}C-PIB PET and ^{18}F-FDG-PET for detection of Alzheimer's disease.** *J Nucl Med* 2007;48:547–52
7. Tolboom N, van der Flier WM, Boverhoff J, et al. **Molecular imaging in the diagnosis of Alzheimer's disease: visual assessment of [^{11}C]PIB and [^{18}F]FDDNP PET images.** *J Neurol Neurosurg Psychiatry* 2010;81:882–84
8. Rabinovici G, Rosen H, Alkalay A, et al. **Amyloid vs FDG-PET in the differential diagnosis of AD and FTLD.** *Neurology* 2011;77:2034–42
9. Iwatsubo T. **Japanese Alzheimer's Disease Neuroimaging Initiative: present status and future.** *Alzheimers Dement* 2010;6:297–99
10. McKhann G, Drachman D, Folstein M, et al. **Clinical diagnosis of Alzheimer's disease: report of the NINCDS-ADRDA Work Group under the auspices of Department of Health and Human Services Task Force on Alzheimer's Disease.** *Neurology* 1984;34:939–44
11. Ikari Y, Nishio T, Makishi Y, et al. **Head motion evaluation and correction for PET scans with ^{18}F-FDG in the Japanese Alzheimer's Disease Neuroimaging Initiative (J-ADNI) multi-center study.** *Ann Nucl Med* 2012;26:535–44
12. Silverman DH, Mosconi L, Ercoli L, et al. **Positron emission tomography scans obtained for the evaluation of cognitive dysfunction.** *Semin Nucl Med* 2008;38:251–61
13. Landis JR, Koch GG. **The measurement of observer agreement for categorical data.** *Biometrics* 1977;33:159–74
14. Lehman VT, Carter RE, Claassen DO, et al. **Visual assessment versus quantitative three-dimensional stereotactic surface projection fluorodeoxyglucose positron emission tomography for detection of mild cognitive impairment and Alzheimer disease.** *Clin Nucl Med* 2012;37:721–26
15. Foster NL, Heidebrink JL, Clark CM, et al. **FDG-PET improves accuracy in distinguishing frontotemporal dementia and Alzheimer's disease.** *Brain* 2007;130(pt 10):2616–35
16. Ishii K, Soma T, Kono AK, et al. **Comparison of regional brain volume and glucose metabolism between patients with mild dementia with Lewy bodies and those with mild Alzheimer's disease.** *J Nucl Med* 2007;48:704–11

Ann Nucl Med (2013) 27:452–459
DOI 10.1007/s12149-013-0704-x

ORIGINAL ARTICLE

Equal sensitivity of early and late scans after injection of FDG for the detection of Alzheimer pattern: an analysis of 3D PET data from J-ADNI, a multi-center study

Ryuichi Takahashi · Kazunari Ishii · Michio Senda · Kengo Ito · Kenji Ishii · Takashi Kato · Yoko Makishi · Tomoyuki Nishio · Yasuhiko Ikari · Takeshi Iwatsubo · Japanese Alzheimer's Disease Neuroimaging Initiative

Received: 26 October 2012 / Accepted: 11 February 2013 / Published online: 13 March 2013

Abstract
Objective To determine the optimal accumulation time for three-dimensional positron emission tomography (3D-PET) with ^{18}F-2-fluoro-2-deoxy-D-glucose (^{18}F-FDG) to detect the brain uptake pattern typical of Alzheimer's disease (AD).
Methods Patients with mild AD or amnestic mild cognitive impairment (MCI) and normal control subjects were recruited in the Japanese Alzheimer's disease neuroimaging initiative and examined with a PET scan during the 30–60 min after FDG injection. Three independent blinded experts interpreted the 30- to 60-min sum images, and images of patients with AD and MCI presenting AD patterns and normal subjects presenting normal patterns were used in the analysis. Early-scan (ES) and late-scan (LS) images were obtained from the data acquired at 30–35 min and 55–60 min after the injection, respectively. Separate target regions of interest (ROI) for ES and LS were defined as areas of significant reductions in the posterior cingulate and parietotemporal lobe in both hemispheres from the results of an initial cohort with 21 patients (AD 16, MCI 5) and 19 controls. A subsequent sample of 36 (AD 9, MCI 27) patients and 38 controls were used to compare the diagnostic capability of ES and LS using *Z* scores within the target ROI in individual statistical parametric mapping analysis.
Results Compared to LS, ES showed lower activity in the frontal lobes and higher activity in the venous sinus than LS; however, the diagnostic capability of ES and LS did not significantly differ (sensitivity 0.97 and 0.97, specificity 0.82 and 0.84, area under the receiver-operating characteristic curve 0.96 and 0.97, respectively).
Conclusions For a qualitative diagnosis of the AD pattern in 3D FDG-PET, results of ES were equivalent to those of LS. ES may be an option to shorten the entire PET procedure time, particularly in diagnosing early stages of AD.

Keywords Alzheimer's disease · Voxel · Accumulation time · PET · 3D

R. Takahashi · K. Ishii · M. Senda · K. Ito · K. Ishii · T. Kato · Y. Makishi · T. Nishio · Y. Ikari
J-ADNI PET core
URL: http://www.j-adni.org/

R. Takahashi (✉)
Department of Neurology, Hyogo Prefectural Rehabilitation Hospital at Nishi-Harima, Kohto 1-7-1 Shingu-cho, Tatsuno, Hyogo 679-5165, Japan
e-mail: r_takahashi@hwc.or.jp

K. Ishii
Department of Radiology, Kinki University Faculty of Medicine, Osakasayama, Osaka, Japan

M. Senda · Y. Makishi · T. Nishio · Y. Ikari
Division of Molecular Imaging, Institute of Biomedical Research and Innovation, Kobe, Japan

K. Ito · T. Kato
Department of Brain Sciences and Molecular Imaging, National Institute for Longevity Sciences, National Center for Geriatrics and Gerontology, Obu, Japan

K. Ishii
Positron Medical Center, Tokyo Metropolitan Institute of Gerontology, Tokyo, Japan

T. Iwatsubo
Department of Neuropathology and Neuroscience, Graduate School of Pharmaceutical Sciences, The University of Tokyo, Tokyo, Japan

Introduction

^{18}F-2-fluoro-2-deoxy-D-glucose (FDG)-positron emission tomography (PET) plays a major role in the early diagnosis of Alzheimer's disease (AD); glucose hypometabolism in the posterior cingulate and parietotemporal lobe is reported to be features of the typical AD pattern [1, 2]. For quantification of glucose metabolic rate, the optimal accumulation time for FDG-PET scan has historically been considered to be 45–55 min after injection or later to allow for phosphorylation of FDG within the brain tissue [3–5]. A number of studies have attempted to determine the optimal accumulation time for detecting AD patterns using two-dimensional (2D) PET scans for qualitative diagnostic purposes. A comparison between scans obtained at 30–42 min and 60–72 min after injection revealed superiority of the latter scan for AD detection [6]. Another study compared scans obtained at 40–50 min and 60–63 min after injection and indicated that the short, late scan was equally capable of detecting AD [7]. Both studies suggest that as accumulation time increased, ^{18}F-FDG uptake increased in the posterior cingulate and parietal cortices (regions affected in AD) and decreased in the cerebellum, providing higher signal-to-noise ratio (S/N) in the later scans.

In recent years, three-dimensional (3D) ^{18}F-FDG-PET has been used in large multicenter neuroimaging studies such as the Alzheimer's disease neuroimaging initiative (ADNI) because of the high sensitivity, short scanning time, and low radiation exposure of this technique. If acquired in 3D, earlier scans may be equally effective for qualitative diagnostic purposes because of the high sensitivity of the technique. Increases in counts from a 3D scan due to high sensitivity leads to decreased noise, which might give a sufficient S/N and detection capability even if the contrast between the hypometabolic region and the normal area is smaller in an early scan (ES) than a late scan (LS). However, the optimal accumulation time to detect AD in 3D PET with ^{18}F-FDG has not been investigated, especially in multicenter studies. The aim of this study was to determine the optimum accumulation time for 3D PET with ^{18}F-FDG by comparing AD detection sensitivity between ES and LS using data from the Japanese ADNI (J-ADNI).

Materials and methods

Subjects

As part of the J-ADNI study, subjects were recruited as patients [clinical mild AD or amnestic MCI (mild cognitive impairment)] or normal controls from 38 clinical sites; imaging was performed for these subjects during 30–60 min after injection of FDG at 24 participating imaging facilities [8]. Three independent experts blinded to the clinical information of the participants, except age, sex, and findings of magnetic resonance imaging, visually classified the FDG uptake pattern of the 30- to 60-min sum images based on the criteria proposed by Silverman and colleagues [1], and the results were subjected to a consensus read. In the present study, PET images of patients with AD and amnestic MCI that classified as an AD pattern (P1 pattern) were used as *affected* images, whereas PET images of normal subjects classified as normal pattern (N1 pattern) were used as *unaffected* images. Imaging results of the first 21 patients and 19 controls were used to determine regions of interest (ROI) for ES and LS, and imaging results of the subsequent 36 patients and 38 controls were evaluated for diagnostic capability using the pre-defined ROI for ES and LS. The characteristics of the subjects are shown in Table 1. The AD-to-MCI prevalence ratio varied in the course of recruitment, and the mean mini mental state examination (MMSE) score was higher in the test subjects than in the subjects enrolled to determine the ROI. No adjustment was made for this variation, because the test subjects were supposed to have more normal images than the subjects whose images were used to determine the ROI, making the diagnostic test more challenging.

Table 1 Characteristics of the subjects

	Subjects for ROI determination		Subjects for ROC analysis	
	Patients with P1 pattern	Normal controls with N1 pattern	Patients with P1 pattern	Normal controls with N1 pattern
Gender, *n* (F/M)	10/11	10/9	23/13	25/13
Age (years)	74.0 ± 6.5	65.6 ± 5.4	73.1 ± 6.1	66.2 ± 34.0
MMSE	23.1 ± 2.2	29.3 ± 1.1	24.9 ± 2.3	29.2 ± 1.1
Education (years)	12.4 ± 4.5	14.3 ± 3.0	13.0 ± 2.6	13.8 ± 2.6

P1 AD pattern, *N1* normal pattern [1]

PET procedures

In the present study, FDG-PET images were acquired according to the standardized protocol of J-ADNI with 20 different PET scanners (7 Shimazu models, 5 GE models, 5 Siemens models, 2 Toshiba models, and 1 Philips model) at 24 imaging facilities. A 30-min dynamic emission scan, consisting of six 5-min frames, was acquired, starting 30 min after intravenous injection of 185 MBq of ^{18}F-FDG. The subjects were instructed to fast for at least 4 h before

the scan and then asked to lie quietly in a dimly lit room with their eyes open under minimal sensory stimulation.

The patient's blood glucose level was measured before ^{18}F-FDG injection, and if it was greater than 180 mg/dL (9.9 mmol/L), the scan was delayed until it fell below 180 mg/dL; if it did not fall below this level, the scan was rescheduled. As a result, the glucose level before injection was 94 ± 19 mg/dL.

Data were corrected for attenuation using a transmission scan or X-ray computed tomography, and the images were reconstructed with an iterative reconstruction algorithm specifically determined for each type of scanner, which provided spatial and axial resolution in the range of 6- to 8-mm FWHM.

Each dynamically acquired image was pre-processed by the J-ADNI PET QC core at the Institute of Biomedical Research and Innovation (Kobe, Japan). An automated algorithm was used to correct for motion between six 5-min emission frames before summation to construct one 30-min emission image, followed by alignment onto a 160 × 160 × 96 matrix of 1.5-mm voxels parallel to the anterior and posterior commissures. Frames presenting large intra-frame motion were discarded as described elsewhere [9]. These images, together with their three-dimensional stereotactic surface projection (3D-SSP) *Z* score images [10], were assessed independently by 3 blinded experts who then discussed the findings and reached a consensus concerning classification. The images were classified into 7 categories as defined by Silverman et al., in which an AD pattern was labeled as P1 and a normal pattern was labeled as N1. In the present study, images of patients with AD and amnestic MCI classified as P1 (*affected*: 33 of 36 ADs and 39 of 56 amnestic MCIs) and those of normal subjects classified as N1 (*unaffected*: 64 of 80) were used. Images with substantial motion were removed; therefore, data from 57 P1 subjects (25 ADs and 32 amnestic MCIs) and 57 N1 subjects were used for the analysis.

The first (30–35 min) and last (55–60 min) frames of the emission scan were extracted as ES and LS, respectively, and were aligned into 160 × 160 × 96 matrix images in the same way as described above.

Image comparison between ES and LS as well as between patients and controls

Anatomical normalization and statistical processing of the PET images were performed using statistical parametric mapping version 8 software for Windows (SPM 8; Wellcome Trust Centre for Neuroimaging, University College London, London, UK). The calculations and image matrix manipulations were performed using MATLAB R2009b (MathWorks Inc., Natick, MA, USA). All individual PET images were transformed into a standard stereotactic anatomical space. Further, all images were smoothed with an isotropic 12-mm Gaussian kernel to increase S/N and compensate for the differences in the gyral anatomy between individuals. The uptake values in individual FDG images were adjusted by proportional scaling to an arbitrary mean value of 5.0. Comparisons between results of ES and LS for the *affected* and *unaffected* groups were analyzed separately by paired *t* tests, and a family-wise error (FWE) corrected threshold of $p < 0.05$ was applied to indicate statistical significance. Comparisons between the results for patients and controls for both ES and LS were analyzed separately by unpaired *t* tests, and an uncorrected threshold of $p < 0.001$ was applied.

ROI determination

Hypometabolic regions were extracted by comparison between *affected* and *unaffected* images for each ES and LS image separately, using the anatomical standardization technique described above and analyzed with unpaired *t* tests with an uncorrected threshold of $p < 0.001$. Out of the voxels presenting significant hypometabolism, those within the posterior cingulate gyrus, precuneus, and parietotemporal lobe were selected in both ES and LS based on previous studies which investigated the early detection of AD and MCI [11–13]. ROI were extracted using Marsbar (http://marsbar.sourceforge.net/).

Comparison of diagnostic capability between ES and LS

For evaluating the diagnostic capability, *Z* score maps were quantitatively analyzed using a free software, Easy *Z* score Imaging System (eZIS; Fujifilm RI Pharma, Tokyo, Japan), which works based on SPM algorithms. Regional glucose metabolic values were obtained as the FDG uptake normalized by the value for the cerebellum and for the whole brain. For these 2 normalized metabolic maps, *Z* scores were calculated for each voxel of each subject's image using the 19 normal control images as a normal database: *Z* score = [(normal mean) − (individual value)/(normal standard deviation, SD)]. The sum of the *Z* scores in the ROI was calculated for the 2 *Z* score maps of the subjects. Receiver-operating characteristic (ROC) analysis was performed, and the area under the ROC curve (AUC) values and their standard errors (SE) were calculated using JROCKIT 1.0.2 software (Department of Radiology and Radiological Science, Johns Hopkins University, Baltimore, Maryland, USA: http://www.rad.jhmi.edu/jeng/javarad/roc/JROCFITi.html).

The jackknife method using LABMRMC software (Department of Radiology, University of Chicago: http://metz-roc.uchicago.edu/) was applied to compare AUCs for ES and LS.

Results

Group differences between ES and LS

Figure 1 shows the metabolic differences between ES and LS. In both *affected* patients and *unaffected* controls, radioactivity distribution in the venous sinus was significantly grater in ES than in LS, and FDG uptake in both the frontal lobes and parts of the parietal lobes was significantly higher in LS than in ES ($P < 0.05$ FWE corrected). Although differences were found in similar regions of *affected* and *unaffected* images, regional differences were more pronounced in the *unaffected* images (Fig. 1; Table 2).

Determination of ROI

Both ES and LS showed significant hypometabolism in the posterior cingulate, both the parietotemporal lobes, the

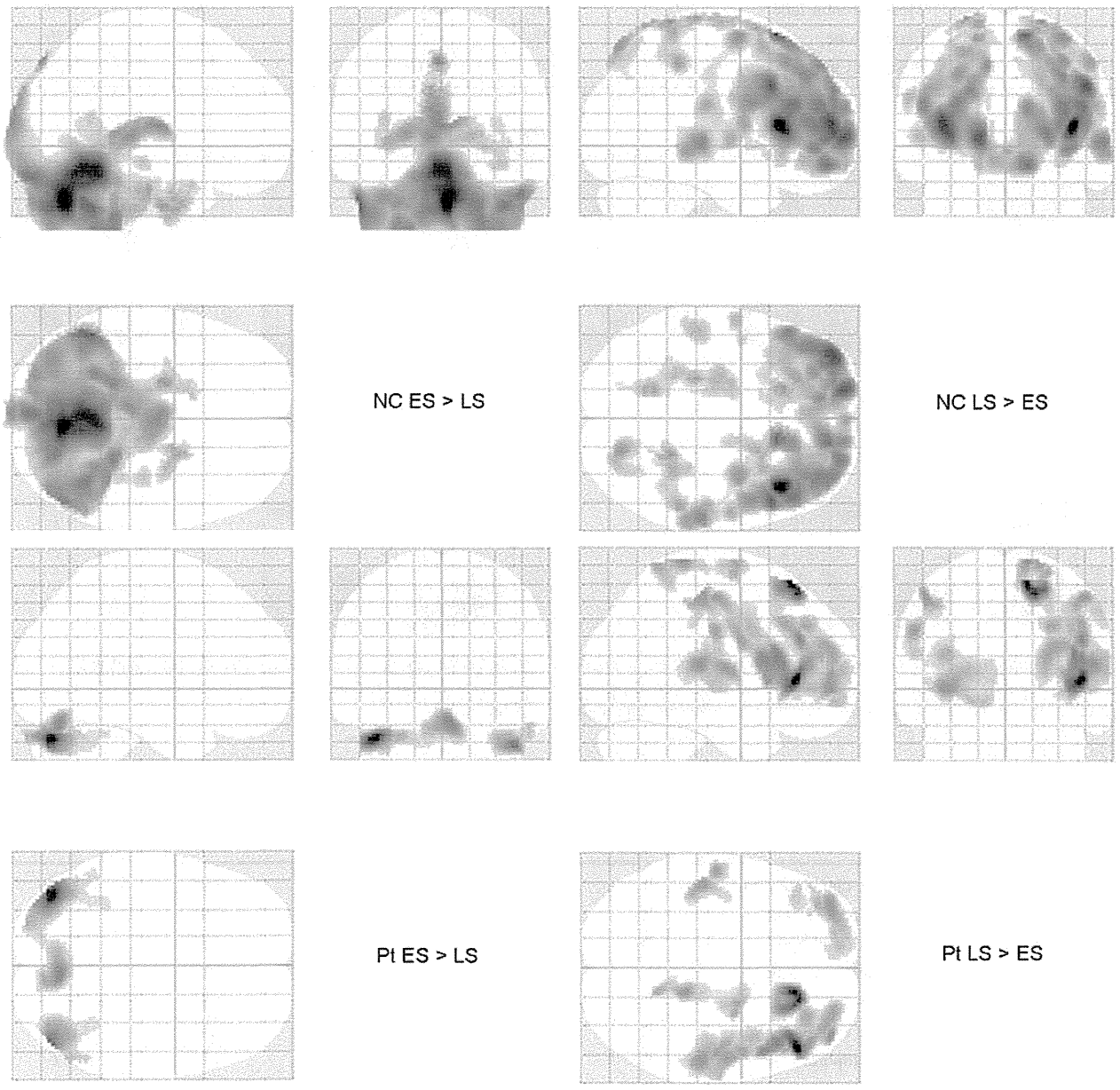

Fig. 1 Areas with significant differences in FDG distribution between ES and LS. In both patients with AD patterns and the normal controls with normal patterns, FDG distribution in the venous sinus was significantly higher in ES, and FDG uptake in the bilateral frontal lobes and part of the parietal lobes was significantly higher in LS ($p < 0.05$ FWE corrected). (*ES* early scan, *LS* late scan, *NC* normal controls with normal pattern, *Pt* patients with AD pattern)

medial frontal lobes, and the insular cortices in the *affected* patient group in comparison to the *affected* control group ($p < 0.001$ uncorrected, Fig. 2). As shown in Table 3, the peak t value for the right posterior cingulate gyrus was 9.05 for ES and 8.93 for LS. For both ES and LS, significantly hypometabolic voxels were extracted from the posterior

Table 2 Regions with significant differences in FDG uptake between ES and LS

Scanning time	Brain region	Talairach coordinates				t value	Voxel extent
		Side	x	y	Z		
ES > LS	Venous sinus	L	−3	−68	−25	19.57	21878
LS > ES	Inferior frontal gyrus	R	40	22	14	11.36	16383
	Medial frontal lobe	L	−16	57	2	7.89	309
	Parietal lobe	L	−23	−40	66	7.87	520
	Precentral gyrus	L	−25	−23	68	7.54	681

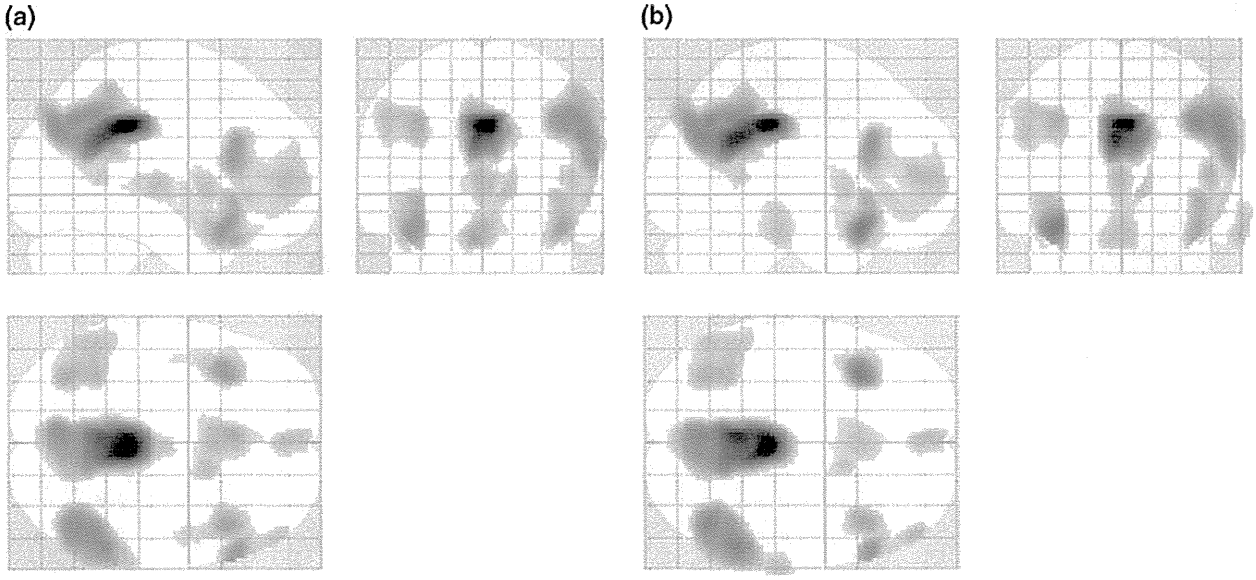

Fig. 2 *Highlighted areas* with significantly lower glucose metabolism in patients with AD pattern than in controls with normal pattern ($p < 0.001$, uncorrected). Bilateral precuneus, posterior cingulate gyrus, parietotemporal lobe, lateral frontal lobes, and medial frontal lobe were *highlighted* in both ES (**a**) and LS (**b**) (*ES* early scan, *LS* late scan)

Table 3 Hypometabolic regions in patients with AD pattern compared with those in normal controls with normal pattern

Scanning time	Brain region	Talairach coordinates				t value	Voxel extent
		Side	x	y	z		
ES	Posterior cingulate gyrus	R	4	−32	34	9.05	4138
	Parietotemporal lobe	R	56	−46	31	5.86	2974
	Middle frontal gyrus	R	56	25	27	5.38	1721
	Parietotemporal lobe	L	−36	−65	34	4.80	1375
	Medial frontal gyrus	L	−2	49	6	4.45	681
LS	Posterior cingulate gyrus	R	2	−30	34	8.93	4243
	Parietotemporal lobe	R	56	−46	31	6.25	3089
	Middle frontal gyrus	R	56	24	27	5.59	1435
	Parietotemporal lobe	L	−36	−63	36	4.71	1345
	Medial frontal gyrus	L	−2	49	7	4.49	577

ES early scan, *LS* late scan

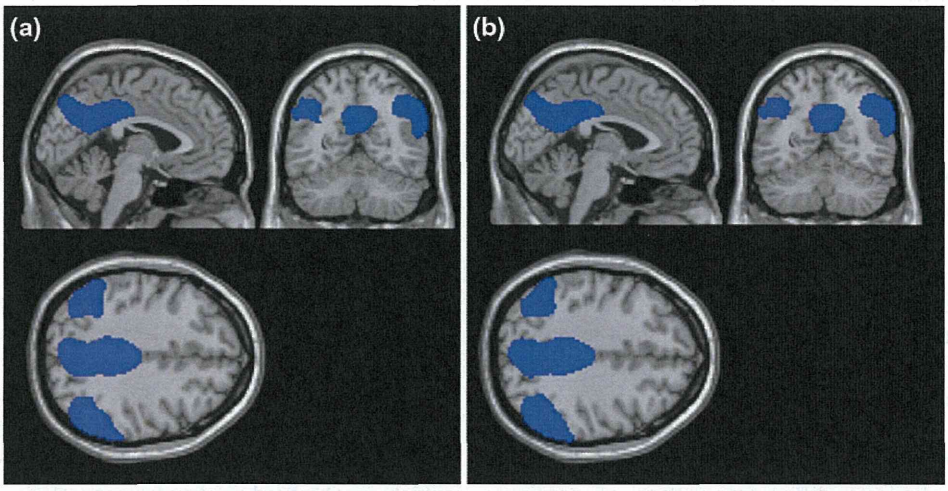

Fig. 3 Target ROI in ES (**a**) and LS (**b**). In both ES and LS, bilateral precuneus, posterior cingulate gyrus, parietotemporal lobe, lateral frontal lobes, and medial frontal lobe were determined as target ROI based on hypometabolic regions observed in patients with AD pattern as compared with controls with normal pattern (*ES* early scan, *LS* late scan)

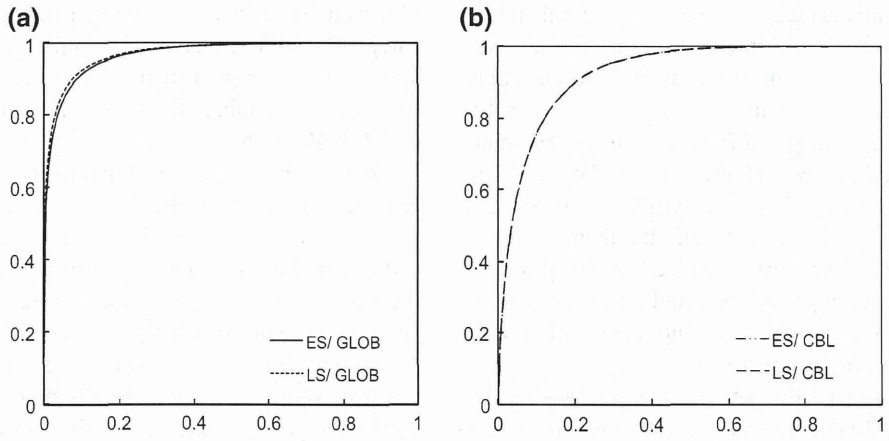

Fig. 4 ROC curves in ES and LS for the detection of AD patterns are shown. ROC curves calculated by the sum of *Z* scores normalized with that of global cerebral metabolism are shown in **a**. ROC curves calculated by the sum of *Z* scores normalized with that of cerebellum are shown in **b**. When normalized with *Z* scores of the whole brain, AUC of ES was 0.972 and AUC of LS was 0.969. When normalized with *Z* scores of the cerebellum, AUC of both ES and LS was 0.925 (*ES* early scan, *LS* late scan, *ROC* receiver-operating characteristic, *AUC* area under curve)

cingulate gyrus, precuneus, or bilateral parietotemporal lobes and were defined as ROI to be used in the analysis of diagnostic capability (Fig. 3).

Comparison of diagnostic capability

Figure 4 shows the ROC curves for ES and LS regarding the diagnostic capability of the sum of *Z* scores within the ROI for the images showing FDG uptake normalized by the whole brain (Fig. 4a) and by the cerebellum (Fig. 4b). When normalized by the whole brain, the AUC for ES was 0.972 and that for LS was 0.969. When normalized by the cerebellum, the AUC was 0.925 for both ES and LS. The AUCs for ES did not significantly differ from those for LS ($p = 0.7676$ when normalized by the whole brain, $p = 0.9931$ when normalized by the cerebellum).

Discussion

To our knowledge, this is the first multicenter analysis study to determine the optimal accumulation time for 3D-PET with ^{18}F-FDG by comparing the sensitivity for AD pattern detection between ES and LS. First, we found no significant differences in the AUCs of ES and LS. Second, in both *affected* patients and *unaffected* controls, ES

showed higher radioactivity in the venous sinus, whereas LS showed higher FDG uptake in both the frontal lobes and parts of the parietal lobes. ES and LS did not show significant differences in the precuneus, posterior cingulate gyrus, and parietotemporal lobes. These results suggest that an accumulation time of 30 min is sufficient for a qualitative diagnosis of AD patterns using 3D PET-FDG images. This result may be applicable to the qualitative diagnosis of hypometabolic patterns in conditions other than AD. Considering that PET department personnel as well as from other healthcare staff are required to provide special care to patients with dementia or other cognitive disorders, reducing the total PET procedure time using ES may reduce the burden on such patients and save the resources of the PET facility.

The current findings differ from those of previous studies that compared early and late scans for 2D PET [6, 7]. This is attributed to the difference in the regional rate of FDG accumulation during the types of PET. The previous studies found that the relative FDG uptake in the posterior cingulate gyrus, precuneus, and parietotemporal lobes, which are the target regions in the detection of AD, was higher in LS than in ES. In contrast, the present study found no particular increase in these regions between ES and LS. There are 3 major differences in the methods between the current study and previous studies that can explain this discrepancy. The first possible explanation may be that 3D PET is more sensitivity than 2D PET. However, the discrepancy was localized in the posterior cingulate and parietotemporal lobes, and was not observed in other cortical regions. The second explanation may involve differences in the resting state during the accumulation and scanning period between the previous studies and this study by J-ADNI. The subjects were required to be awake with their eyes open during the FDG accumulation period in the current study but not in the previous studies. This may have influenced consciousness during scanning and modified the results. The posterior cingulate gyrus, precuneus, and parietotemporal lobes are reported to be the main components of the default-mode network, which is a consistent brain activity of the passive resting state that decreases on cognitive processing [14, 15]. The state of open eyes influences the default-mode network, which may lead to a decrease in neuronal activity in these areas. Therefore, the difference in these areas between ES and LS might diminish when the eyes are open as compared to when they are closed. However, this hypothesis has not been confirmed and requires further investigation. In future multicenter studies, eye opening/closing during the FDG accumulation period may be taken into account. The third explanation may be the multicenter nature of the study design. As the J-ADNI project is a multicenter study, various kinds of PET scanners were included in the analysis. However, the scanning protocols were strictly standardized, and the J-ADNI PET QC core determined the details of data acquisition for each PET camera model to minimize the camera-derived difference [9]. Furthermore, the quality of all images was confirmed by the PET QC core after they were acquired. Therefore, we do not think that this factor was the cause of the above-mentioned discrepancy.

The increase in FDG uptake from ES to LS in the frontal lobes was similar to the results reported by Sakamoto and colleagues [6]. Interestingly, the difference between ES and LS in this region was more pronounced in normal *unaffected* control subjects than in *affected* patients. This suggests that the sensitivity differences of LS and ES may be important in detecting frontal lobe hypometabolism, which is observed in frontotemporal dementia and progressive supranuclear palsy. However, because these areas were outside the ROI in this study, this finding did not influence the detection of AD pattern.

The decrease in radioactivity in the venous sinus observed by us was not reported in previous studies. In early FDG-PET scans, a substantial amount of ^{18}F-FDG still exists in the pool of the venous sinus; the high sensitivity of 3D scanning may have contributed to the detection of ^{18}F-FDG in the sinus area.

Despite the important findings of this study, a few important limitations should be noted. There was a significant difference in age between the patients and control subjects in this study. During early recruitment for J-ADNI, the normal controls were younger than the patients (the subjects were not randomly sampled). Therefore, the more prominent differences between ES and LS for normal controls compared to patients may potentially be caused by their younger age. However, this difference should not influence the diagnostic value of ES for AD, because these findings were observed outside the ROI. Lastly, we did not examine the diagnostic performance of the full 30-min scan because the focus of this study was a comparison between ES and LS and a 30-min scan may be too long for a routine clinical scan.

In conclusion, the present study provides evidence that 3D-PET ES may be sufficient to detect AD pattern. ES may be used to shorten the entire PET procedure time to reduce the burden on the patients and to save the resources of the facility. However, the differences in the radioactivity changes in the frontal lobes and venous sinus between ES and LS should be considered.

Acknowledgments This study is a part of the "Translational Research Promotion Project/Research project for the development of a systematic method for the assessment of Alzheimer's disease," sponsored by the New Energy and Industrial Technology Development Organization (NEDO) of Japan. J-ADNI is also supported by a Grant-in-Aid for Comprehensive Research on Dementia from the

Japanese Ministry of Health, Labour and Welfare, as well as by the grants from J-ADNI Pharmaceutical Industry Scientific Advisory Board (ISAB) companies. The authors would also like to thank the J-ADNI Imaging ISAB and other organizations for their support of this work.

Conflict of interest The authors report no conflict of interest.

References

1. Silverman DH, Small GW, Chang CY, Lu CS, Kung De Aburto MA, Chen W, et al. Positron emission tomography in evaluation of dementia: regional brain metabolism and long-term outcome. JAMA. 2001;286:2120–7.
2. Minoshima S, Giordani B, Berent S, Frey KA, Foster NL, Kuhl DE. Metabolic reduction in the posterior cingulate cortex in very early Alzheimer's disease. Ann Neurol. 1997;42:85–94.
3. Phelps ME, Huang SC, Hoffman EJ, Selin C, Sokoloff L, Kuhl DE. Tomographic measurement of local cerebral glucose metabolic rate in humans with (F-18)2-fluoro-2-deoxy-D-glucose: validation of method. Ann Neurol. 1979;6:371–88.
4. Lucignani G, Schmidt KC, Moresco RM, Striano G, Colombo F, Sokoloff L, et al. Measurement of regional cerebral glucose utilization with fluorine-18-FDG and PET in heterogeneous tissues: theoretical considerations and practical procedure. J Nucl Med. 1993;34:360–9.
5. Schmidt KC, Lucignani G, Sokoloff L. Fluorine-18-fluorodeoxyglucose PET to determine regional cerebral glucose utilization: a re-examination. J Nucl Med. 1996;37:394–9.
6. Sakamoto S, Ishii K, Hosaka K, Mori T, Sasaki M, Mori E. Detectability of hypometabolic regions in mild Alzheimer disease: function of time after the injection of 2-[fluorine 18]-fluoro-2-deoxy-D-glucose. AJNR Am J Neuroradiol. 2005;26:843–7.
7. Chen WP, Matsunari I, Noda A, Yanase D, Yajima K, Takeda N, et al. Rapid scanning protocol for brain (18)F-FDG PET: a validation study. J Nucl Med. 2005;46:1633–41.
8. Arai H, Okamura N, Furukawa K, Kudo Y. Geriatric medicine, Japanese Alzheimer's disease neuroimaging initiative and biomarker development. Tohoku J Exp Med. 2010;221:87–95.
9. Ikari Y, Nishio T, Makishi Y, Miya Y, Ito K, Koeppe RA, et al. Head motion evaluation and correction for PET scans with 18F-FDG in the Japanese Alzheimer's disease neuroimaging initiative (J-ADNI) multi-center study. Ann Nucl Med. 2012;26:535–44.
10. Cross DJ, Minoshima S, Nishimura S, Noda A, Tsukada H, Kuhl DE. Three-dimensional stereotactic surface projection analysis of macaque brain PET: development and initial applications. J Nucl Med. 2000;41:1879–87.
11. Arnaiz E, Jelic V, Almkvist O, Wahlund LO, Winblad B, Valind S, et al. Impaired cerebral glucose metabolism and cognitive functioning predict deterioration in mild cognitive impairment. NeuroReport. 2001;12:851–5.
12. Herholz K, Salmon E, Perani D, Baron JC, Holthoff V, Frolich L, et al. Discrimination between Alzheimer dementia and controls by automated analysis of multicenter FDG PET. Neuroimage. 2002;17:302–16.
13. Drzezga A, Lautenschlager N, Siebner H, Riemenschneider M, Willoch F, Minoshima S, et al. Cerebral metabolic changes accompanying conversion of mild cognitive impairment into Alzheimer's disease: a PET follow-up study. Eur J Nucl Med Mol Imaging. 2003;30:1104–13.
14. Fair DA, Schlaggar BL, Cohen AL, Miezin FM, Dosenbach NU, Wenger KK, et al. A method for using blocked and event-related fMRI data to study "resting state" functional connectivity. Neuroimage. 2007;35:396–405.
15. Raichle ME, MacLeod AM, Snyder AZ, Powers WJ, Gusnard DA, Shulman GL. A default mode of brain function. Proc Natl Acad Sci USA. 2001;98:676–82.

老年精神医学雑誌　第24巻第7号(2013.7)別刷

基礎講座

老年精神医学と Brain Imaging ⑦

アルツハイマー病の画像診断

伊藤健吾・加藤隆司・文堂昌彦・中村昭範

基礎講座　老年精神医学とBrain Imaging

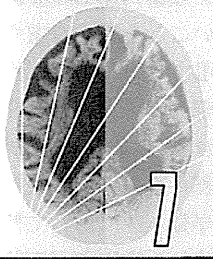

アルツハイマー病の画像診断

伊藤健吾，加藤隆司，文堂昌彦，中村昭範

老年精神医学雑誌 24：707-714，2013

はじめに

アルツハイマー病（Alzheimer's disease；AD）の診断では，CTとMRIが正常圧水頭症，慢性硬膜下血腫など外科的治療で治癒可能な認知症の除外診断と脳血管障害の評価において必須とされてきたが，脳血流SPECTと糖代謝FDG-PET（以下，FDG-PET）などの機能的診断法は，補助診断法と位置づけられてきた．しかし，患者数が飛躍的に増加するなかで，より精度の高い診断が求められるとともに，アミロイドPETなど画像診断技術の進歩により，ADの診断における画像診断の位置づけは大きく変化した．

2011年，27年ぶりにADの臨床診断基準NINCDS-ADRDAが改訂されたが，これまでのADの診断基準に加えて，軽度認知障害（mild cognitive impairment；MCI）の段階と発症前（preclinical）の段階での診断基準（preclinicalの段階については臨床研究専用）が提案された．いずれの段階においてもMRI，FDG-PET，アミロイドPETが髄液のアミロイドβタンパク（Aβ），タウ（τ）とともにバイオマーカーとして診断基準に組み入れられた[1,9,13,19]．

改訂されたADの診断基準においても，画像バイオマーカーの情報なしでの臨床診断は可能であるが，より確信度の高い診断を必要とする場合には，MRI，脳血流SPECT，FDG-PET，アミロイドPETを積極的に活用していくことになる．ただし，前述の新診断基準の解説でも述べられているように，診断基準に新たに導入されたバイオマーカーそれぞれのあるいはそれらを組み合わせた場合の有用性についてはまだ検討の余地があることも事実である．そのためにADNI（Alzheimer's Disease Neuroimaging Initiative）などの臨床研究が進められている．

本稿では，ADの診断における画像バイオマーカーとしてのMRI，脳血流SPECT，FDG-PET，アミロイドPETの最近の進歩を踏まえて，ADの診断におけるこれらの画像バイオマーカーの有用性と位置づけについて述べる．

Ⅰ．もの忘れセンターにおける画像診断

筆者らの所属する施設は認知症疾患医療センターに認定されているが，その中核として「もの忘れセンター」が設置されている．「もの忘れセンター」では月曜日から金曜日までの連日，午前と午後に外来診療が行われ，初診患者は年間1,000例以上を超えるため，数多くの画像診断が実施されている．MRIが禁忌の場合を除き，全例でMRIが実施され，側頭葉内側部の萎縮を含めて脳の形態学的な評価が行われる．海馬および海馬近傍の萎縮の客観的評価のためには，VSRAD®（Voxel-based Specific Regional analysis system for Alzheimer's Disease）による画像統計解析が全例で実施されている．MRIの評価により，認知症の

Kengo Ito, Takashi Kato, Masahiko Bundo, Akinori Nakamura：国立長寿医療研究センター病院放射線診療部／認知症先進医療センター脳機能画像診断開発部
〒474-8522　愛知県大府市森岡町源吾35

診断に関する多くの情報が得られるが，鑑別診断を含む基本的な評価に加えて，ADを疑う場合には，側頭葉内側部の萎縮が他部位の萎縮に比べて目立つこと，65歳以下の若年発症であれば側頭葉内側部の萎縮が比較的目立たないこと，重複する病態（脳血管障害，特発性正常圧水頭症など）の存在などに注意して診断を進める．

MRIでADが疑われた場合，進行したADで検査を追加する臨床的意義が乏しい場合や，検査の実施が困難な場合を除き，脳血流SPECTが実施される．脳血流SPECTよりもFDG-PETのほうが診断能が高いことは証明されているが，日本ではFDG-PETは認知症を対象とした場合には保険適用外となるため，原則的に脳血流SPECTが選択される．FDG-PETおよびアミロイドPETは，主に臨床研究の枠内で実施されている．

高齢者では，ADを示唆する脳血流SPECTの所見が若年者に比べて出にくいことに留意すべきであるが，脳血流SPECTでADに典型的な所見が得られれば，ADの確信度は高くなる．もし，レビー小体型認知症（dementia with Lewy bodies；DLB）を示唆する後頭葉内側部の血流低下のように他の認知症を示唆する所見が得られた場合には，改めて病歴，臨床所見，神経心理検査，MRIを再検討するとともに必要に応じて^{123}I-MIBG心筋シンチグラフィーなどの検査を追加することになる．

Ⅱ．MRIによる診断

MRIにより，ADとAD以外の認知症（non-AD）を鑑別する場合に，non-ADの特徴的な萎縮を見逃さない必要があるが，ADを検出する感度の観点からは，側頭葉内側部の萎縮の評価が主体となる．最近のレビュー[2]では，MRIによるADとnon-ADの診断能は，MCI段階の早期を含めても，感度84%，特異度74%と報告されている．しかし，評価に用いられた論文で使用されている萎縮の評価法には，目視での輪郭設定による容積測定など，日常臨床で実施することが困難なものが含まれている．また，側頭葉内側部の萎縮がADに特異的なものではないことを常に考慮する必要がある．VSRAD®を使用すると，内側側頭部（海馬・扁桃・嗅内野の大部分）の萎縮の程度がZ-scoreという数値で示されるのみでなく，脳全体の萎縮の程度，内側側頭部の萎縮の特異性などを評価できる．VSRAD®は早期ADにおいて健常高齢者との比較では80%以上の識別率（正診率）となることが確認されているが[11]，その使用にあたっては，VSRAD®の処理過程でエラーを生じる可能性もゼロではないことに十分に注意して使用する必要がある．

後述するADNIでは，MRIの画像処理，解析について多くの方法論的開発が行われ，これまでの関心領域（ROI）解析，VBM（voxel-based morphometry）に加えて，FreeSurfer（http://surfer.nmr.mgh.harvard.edu/）による容積測定，TBM（tensor-based morphometry）やDBM（deformation-based morphometry）などが検討されている．また，画像データから，個々の症例を分類する方法として，SVM（support vector machine）などを応用した手法も使用されている．多くの方法論を組み合わせた多様な解析結果が報告されているが，ADと健常高齢者の間では80%以上の識別率となるものの，MCIと健常高齢者の間では識別率は70%台に低下，MCIからADへの進行予測ではさらに60%台に低下する[21]．一方，進行度の指標としてはMRIによる脳容積測定が最も統計学的検出力に優れており，疾患修飾薬（disease modifying-therapy；DMT）の治験における必要被験者数のシミュレーションでは，他のモダリティと比較して最も少ない被験者で治療効果の判定が可能であることが示されている[21]．とくにMCIを対象とするときにより縮減効果が大きい．

Ⅲ．脳血流SPECTによる診断

ADとnon-ADの鑑別は実際の臨床では困難である場合も多い．またnon-ADには，前頭側頭型認知症（frontotemporal dementia；FTD），レビ

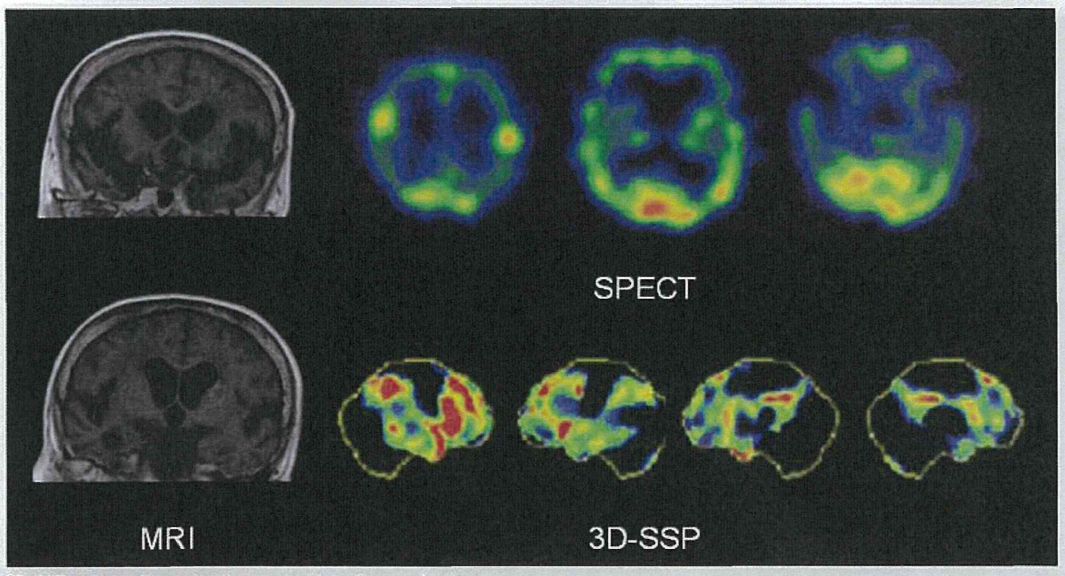

3D-SSP：three-dimensional stereotactic surface projection
MRIでは側脳室の拡大が目立ち（Evans index：0.33），シルビウス裂・脳底槽の拡大を認める．一方，高位円蓋部脳溝・クモ膜下腔は相対的に狭い．脳血流SPECTでは両側側頭・頭頂連合野，楔前部～後部帯状回，前頭葉外側と内側で血流低下を認める．本症例はタップテストも行われ，特発性正常圧水頭症と診断された．ただし，脳血流SPECTではADパターンの血流低下も明らかであり，両疾患の合併症例と考えられた．腰椎－腹腔シャント手術を施行したが，認知機能の改善効果は限定的であった．

図1　特発性正常圧水頭症とアルツハイマー病（AD）の合併と診断された症例

ー小体型認知症（DLB），進行性核上性麻痺（progressive supranuclear palsy；PSP），大脳皮質基底核変性症（corticobasal degeneration；CBD）など多くの疾患が含まれ，それらの間での鑑別も必要となる．SPECTで典型的な画像所見を示す症例では鑑別診断における確信度が増加する．それぞれの疾患におけるSPECT所見の特徴については成書[5,12,20]を参考にされたい．複数の病態が重複する症例が存在することにも注意をはらうべきである．図1に示す症例は特発性正常圧水頭症（idiopathic normal pressure hydrocephalus；iNPH）にADを合併していると考えられた症例である．このような場合も脳血流SPECTの有用性は高い．

^{99m}Tc-HM-PAO SPECTによる研究のメタ解析によると，ADとFTDの鑑別では感度71.5%，特異度78.2%である．また，ADと血管性認知症（vascular dementia；VaD）の鑑別では，感度71.3%，特異度73%と報告されている[3]．^{123}I-IMP SPECTと3D-SSPを用いた研究では，あらかじめ設定したROIをベースにした自動解析で，AD/DLBとnon-AD/DLBの鑑別において感度97%，特異度90%という高い診断能が報告されている[7]．先述の^{99m}Tc-HM-PAO SPECTによる研究のメタ解析において，変性性認知症として頻度が高く，臨床的に鑑別が重要でありながら画像所見が類似しているADとDLBの鑑別では，感度68%，特異度75%と報告され[3]，感度がやや低い．この検討ではDLBにおける後頭葉での集積低下の有無を鑑別の指標としている．

MCIの段階は今後DMTが開発された場合には治療を開始するのにより適切な時期とも考えられることから，MCIの段階で早期診断をする必要性はとくに高い．

脳血流SPECTによるMCIの段階での早期診断は，MCIからADへの進行を確実に予測できるかどうかということになる．図2はMCIからAD

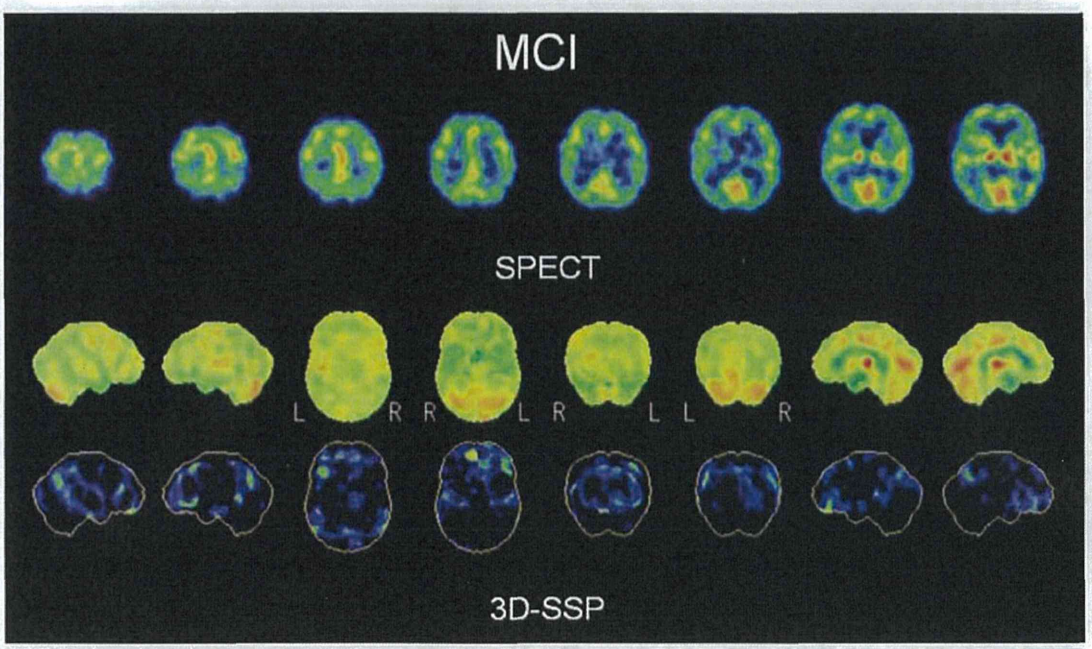

3D-SSP：three-dimensional stereotactic surface projection
本症例はMCIと診断された時点で，両側側頭・頭頂連合野，楔前部～後部帯状回に血流低下が認められたが，その程度は軽度である．脳血流SPECTの3D-SSP上でも全体としてはAD的な血流低下であるが，個々の領域での変化はわずかである．

図2　初診後3年目に軽度認知障害（MCI）からアルツハイマー病（AD）へ進行した症例

への進行例を示す．Yuanら[22]のレビューによれば，脳血流SPECTによるMCIからADへの進行予測について，これまでの論文をまとめた結果では，感度84%，特異度70%と報告されている．ところが，近年日本で行われた多施設共同研究「MCIを対象としたアルツハイマー型痴呆の早期診断に関する研究（Japan Cooperative SPECT Study on Assessment of Mild Impairment of Cognitive Function；J-COSMIC）」（主任研究者：米倉義晴）では，感度76%，特異度39%と報告されており，これまでの成績に比べて特異度がかなり低く，乖離がある．評価法の違いなどを考慮する必要があるが，MCIを対象とする場合には，疑陽性の存在を常に念頭におく必要があると思われる[10]．

Ⅳ．FDG-PETによる診断

FDG-PETは脳血流SPECTより全般的に診断能が高いとされている．変性性認知症として頻度が高く，臨床的に鑑別が重要でありながら画像所見が類似しているADとDLBの鑑別では，それぞれの臨床診断基準により診断された症例を対象として評価した論文をまとめると感度96%，特異度77%となり，特異度がやや低いが感度は高い[8]．また，アメリカではADとFTDの鑑別において臨床診断で鑑別が困難な症例という条件付きながら，FDG-PETがMedicareで保険収載となっている．ADとFTDの鑑別について論文をまとめると感度99%，特異度66%となり，やはり特異度が低い[8]．実際の臨床の状況により則していると判断されるADとVaD，DLB，FTD，その他の種々の認知機能障害を生じる疾患が混在した患者群での検討において，論文をまとめると感度93%，特異度65%である[8]．種々の認知症が混在する状態でも感度は高いが，やはり疑陽性と

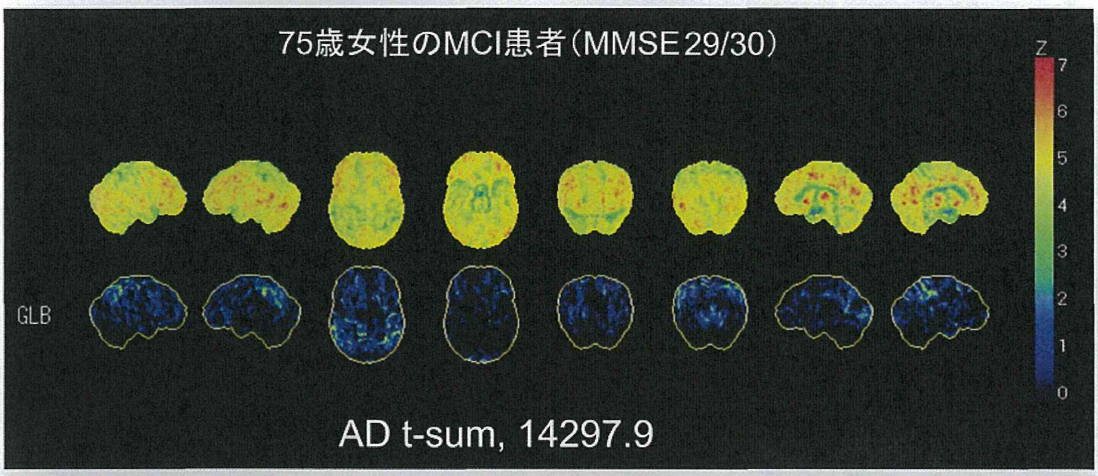

75歳女性のMCI患者（MMSE 29/30）の脳糖代謝PET画像を3D-SSP処理を行うとともに，AD t-sum値を計算した症例．脳糖代謝は，後部帯状回～楔前部，下部頭頂葉に非常に微弱ではあるが低下が認められる．しかし，視察では，確信度は高くないと考えられる．本例のAD t-sumは14297.9で，危険率0.05をクリアして，AD的変化があることが数値上でも示され，ADへの進行が予測された．

図3　AD t-sum算出によりADへの進行が予測された症例

してADと診断される場合がまれではないことに注意する必要がある．

FDG-PETによるMCIの段階での早期診断も，MCIからADへの進行を確実に予測できるかどうかということになる．これまでの論文をまとめると感度79%，特異度89%である[8]．また，FDG-PETによる評価に加えて，アポリポタンパクE（apolipoprotein E；*APOE*）遺伝子型（genotype）を併用するとさらに精度が上がるという報告がある[4,14]．脳血流SPECTと同様に追跡期間が短いと特異度が低くなる可能性があるが，これまでの報告では特異度は高い．日本で行われた多施設共同研究「MCIを対象とするアルツハイマー病の早期診断に関する多施設共同研究（Study on Diagnosis of early Alzheimer's disease-Japan；SEAD-Japan）」（主任研究者：伊藤健吾）では，FDG-PETの予測診断能は，視察では感度95%，特異度47%で，全体の診断能は脳血流SPECTより高かったが，特異度は低い傾向であった．このため，数値評価法としてAD t-sum法[6]を適用して，定量評価を試みた（図3）．AD t-sum値が11,080以上の場合をADと判定した場合，比較的短い2年間での診断能が最も高く，感度73%，特異度88%となり，これまでの報告に近い成績であった．

FDG-PETの結果からは，数値評価法としてAD t-sum法を導入してAD的な糖代謝の低下がよりはっきりした症例を選択することで2年目までの早期に進行する症例を選択することが可能になる．視察でADを疑うが，数値評価法では閾値以下の場合は，3年目以降にコンバートする症例が予想されるので，より長期にわたる追跡が必要であると考えられる．

V．アミロイドPETによる診断

アミロイドPETに使用する放射性薬剤としては，^{11}C-PiB（Pittsburgh Compound-B）が代表的であるが，PiBは^{11}C標識なので半減期が20分であり，院内製剤としてのみ使用可能で，広く普及することは期待できない．このため，^{18}F標識の薬剤が望まれており，^{18}F-AV-45，^{18}F-AV-1，^{18}F-PiBなどの^{18}F標識の薬剤の開発が進んでいる．^{18}F-AV-45のように臨床試験が終了してアメリカ食品医薬品局（FDA）の承認を得た製剤もあり，今後の保険収載が期待されている．

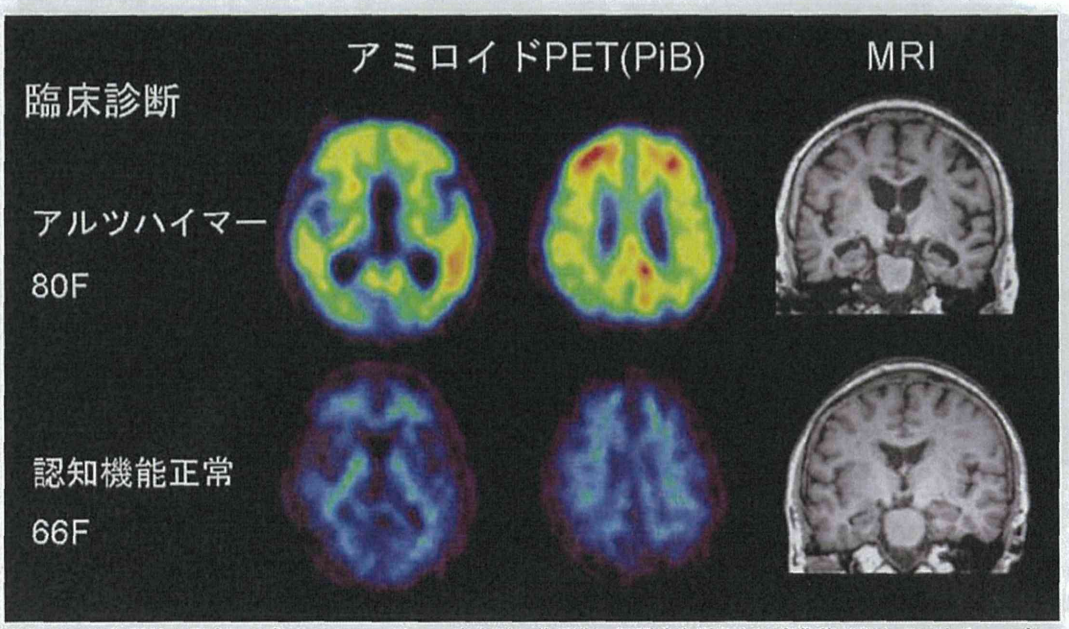

PiB-PETの典型像を示す．上段はアルツハイマー病症例で前頭葉，側頭葉皮質などの高集積が明らかである．一方，下段の健常高齢者では白質に非特異的な軽度集積が認められるのみである．PiB-PETの画像では通常，陽性と陰性の判別が容易である．

図4　PiB陽性と陰性の典型像

^{18}F-AV-45の認可以前に，事実上の標準となっていたのはPiBである．PiBは，アミロイドプラークに対する高い親和性と特異性という優れた特徴をもち，多数の検査が各国で実施された．図4にPiB陽性と陰性の典型像を示す．現在までに集積された*in vivo*アミロイドPETの知見の大半は，PiB-PET検査によるものである．

ADは，最初の症状が記憶障害であるとは限らずFTDを含む前頭側頭葉変性症（frontotemporal lobar degeneration；FTLD）と紛らわしい場合がある．このように，非定型的な発症の認知症の鑑別診断に，病理特異性の高いアミロイドPETが期待される[18]．

ADとFTLDの鑑別に関するFDGとPiBの診断成績の比較研究[16,17]によると，両者はほぼ同等の高い鑑別診断能をもつが，ADを検出する感度はPiBのほうが高く，特異度に関しては，同等ないしFDGのほうが高い．これらの研究は，臨床診断を基準としているためにさらに検証が必要であるが，アミロイドPETのほうがAD病理を検出する感度の高いことは予想された結果である．PiBは有力な検査方法であるが，後述するように課題はあり，臨床症候とPiB所見が対立する場合など，FDGが補完的役割を果たす可能性もある．

DLBではPiBの集積陽性者が多いが，陽性例と陰性例は，レビー小体病のそれぞれcommon form（AD病理を合併する）とpure form（AD病理を合併しない）に対応すると考えることができる．アミロイド病理を併存することが多いDLBの鑑別には，アミロイドPETは有用ではない．

MCIは，AD以外のさまざまな病因を含む可能性がある．Zhangら[23]のメタ解析によると，AD移行予測のプールされた感度と特異度は，PiB-PETがそれぞれ93.5%，56.2%，FDG-PETが78.7%，74.0%であった．PiB-PETは，FDG-PETと比較して，感度は高いが特異度は低い．PiB陽性であることが，短期でのAD発症に結びつくわけではないことを示している．

Ⅵ. ADNIによる画像バイオマーカーの研究

アメリカでは，2005年から北米57施設が参加して，大規模で包括的な前向き臨床研究ADNI（Alzheimer's Disease Neuroimaging Initiative, http://www.Loni.ucla.edu/ADNI）が開始された．この研究は，健常高齢者（NC）200例，MCI 400例，AD 200例という多数の症例集積を行って，MRIによる脳容積測定，PETによる脳代謝画像，アミロイドPETなどの画像マーカーと脳脊髄液，血液などの体液生化学マーカーを6～12か月ごとに縦断的に検討し，臨床・神経心理学評価を組み合わせて，ADの早期診断のみならず，進行評価における有用性を検証し，標準的な評価体系として確立することが目的である．ADNIではADを評価するサロゲートマーカーとしての脳画像，体液生化学マーカーの確立とその標準化を世界的規模で行うことを目指しており，そのために，日本（J-ADNI），ヨーロッパ，オーストラリアなどでも平行してADNIに類似した研究が実施され，順次参加国が増加している（World-wide ADNI）．

被験者の組み入れは，2005年9月より開始され，約2年後の2007年夏にNC 229例，MCI 398例，AD 192例，総計819例で完了した[15]．

2010年秋のADNI終了時に公表された解析結果では，アミロイド指標による臨床的進行の予測について重要な知見が得られた．アミロイドPETについてみると，MCIでは12か月間にPiB陽性群47例中21例（44.7%）がADにコンバートしたのに対し，陰性群は18例中3例（16.7%）にとどまり，高い進行予測能が示された．筆者らがADNIのデータを独自に解析した結果でも，MCIの3年間のコンバート率は，PiB陽性FDG陽性群65.2%，PiB陽性FDG陰性群37.5%，PiB陰性FDG陽性群40%，PiB陰性FDG陰性群12.5%となった．PiB陰性群でのコンバート例は実際にはAD以外の認知症の可能性がある．

このようにバイオマーカーを組み合わることでADにコンバートするリスクが異なる群を分類できることは，2011年に発表されたADの新診断基準[1]の妥当性を示すものである．また，進行度の指標としてはMRIによる脳容積測定が最も統計学的検出力に優れ，FDG-PETはこれに次ぐことが確認された．これらの結果に基づき，MCI症例からアミロイド蓄積の指標（髄液Aβ，アミロイドPET）によりprodromal ADを抽出し，これに対して臨床指標とMRIを組み合わせて薬効評価を行う治験も開始されている．

まとめ

ADの画像診断では，日常診療においてはMRI，脳血流SPECTを疾患の病態を表現するバイオマーカーと位置づけて，その有用性と限界を理解したうえで，早期診断，鑑別診断のために，適切な検査の実施とその結果を正しく評価して診療に活かすことが重要である．まだ認知症について保険適用外のFDG-PETと，現在導入されつつあるアミロイドPETは，ADの早期診断とともに鑑別診断にもきわめて有用であるが，画像バイオマーカーとしては相補的な意味合いをもっている．ただし，これらの画像バイオマーカーの診断成績は報告によりばらつきもあるので，大規模臨床研究ADNI，J-ADNIなどの最終結果が期待される．今後，画像バイオマーカーは薬物あるいは非薬物療法によるADへの早期介入を行う場合に，症例選択および介入による治療効果の判定においても大きな役割が期待される．

文　献

1) Albert MS, DeKosky ST, Dickson D, Dubois B, et al.: The diagnosis of mild cognitive impairment due to Alzheimer's disease ; Recommendations from the National Institute on Aging-Alzheimer's Association workgroups on diagnostic guidelines for Alzheimer's disease. *Alzheimers Dement*, **7** : 270-279 (2011).
2) Bloudek LM, Spackman DE, Blankenburg M, Sullivan SD : Review and meta-analysis of biomarkers and diagnostic imaging in Alzheimer's

disease. *J Alzheimers Dis*, **26** : 627-645 (2011).
3) Dougall NJ, Bruggink S, Ebmeier KP : Systematic review of the diagnostic accuracy of ^{99m}Tc-HMPAO-SPECT in dementia. *Am J Geriatr Psychiatry*, **12** : 554-570 (2004).
4) Drzezga A, Grimmer T, Riemenschneider M, Lautenschlager N, et al.: Prediction of individual clinical outcome in MCI by means of genetic assessment and (18) F-FDG PET. *J Nucl Med*, **46** : 1625-1632 (2005).
5) 橋本　順：脳血流SPECTによる認知症の鑑別診断．臨床放射線，**55**：1386-1407 (2010).
6) Herholz K, Salmon E, Perani D, Baron JC, et al.: Discrimination between Alzheimer dementia and controls by automated analysis of multicenter FDG PET. *Neuroimage*, **17** : 302-316 (2002).
7) Ishii K, Kanda T, Uemura T, Miyamoto N, et al.: Computer-assisted diagnostic system for neurodegenerative dementia using brain SPECT and 3D-SSP. *Eur J Nucl Med Mol Imaging*, **36** : 831-840 (2009).
8) 伊藤健吾，加藤隆司，鳥塚莞爾：公表された文献による18F-FDG PETのアルツハイマー病診断における有用性に関する報告．核医学，**47**：1-8 (2010).
9) Jack CR Jr, Albert MS, Knopman DS, McKhann GM, et al.: Introduction to the recommendations from the National Institute on Aging-Alzheimer's Association workgroups on diagnostic guidelines for Alzheimer's disease. *Alzheimers Dement*, **7** : 257-262 (2011).
10) J-COSMIC実行委員会：J-COSMIC最終報告書．長寿科学振興財団，愛知 (2010).
11) 松田博史：早期アルツハイマー型認知症診断支援システムVSRADについて．日本放射線技術学会雑誌，**62**：1066-1072 (2005).
12) 松田博史，朝田　隆（編）：見て診て学ぶ認知症の画像診断 改訂第2版．永井書店，大阪 (2010).
13) McKhann GM, Knopman DS, Chertkow H, Hyman BT, et al.: The diagnosis of dementia due to Alzheimer's disease ; Recommendations from the National Institute on Aging-Alzheimer's Association workgroups on diagnostic guidelines for Alzheimer's disease. *Alzheimers Dement*, **7** : 263-269 (2011).
14) Mosconi L, Perani D, Sorbi S, Herholz K, et al.: MCI conversion to dementia and the APOE genotype ; A prediction study with FDG-PET. *Neurology*, **63** : 2332-2340 (2004).
15) Petersen RC, Aisen PS, Beckett LA, Donohue MC, et al.: Alzheimer's Disease Neuroimaging Initiative (ADNI) ; Clinical characterization. *Neurology*, **74** : 201-209 (2010).
16) Rabinovici GD, Rosen HJ, Alkalay A, Kornak J, et al.: Amyloid vs FDG-PET in the differential diagnosis of AD and FTLD. *Neurology*, **77** : 2034-2042 (2011).
17) Rostomian AH, Madison C, Rabinovici GD, Jagust WJ : Early 11C-PIB frames and 18F-FDG PET measures are comparable ; A study validated in a cohort of AD and FTLD patients. *J Nucl Med*, **52** : 173-179 (2011).
18) Rowe C, Ng S, Ackermann U, Gong SJ, et al.: Imaging beta-amyloid burden in aging and dementia. *Neurology*, **68** : 1718-1725 (2007).
19) Sperling RA, Aisen PS, Beckett LA, Bennett DA, et al.: Toward defining the preclinical stages of Alzheimer's disease ; Recommendations from the National Institute on Aging-Alzheimer's Association workgroups on diagnostic guidelines for Alzheimer's disease. *Alzheimers Dement*, **7** : 280-292 (2011).
20) 高橋美和子，百瀬敏光：SPECT：主に血流評価による早期診断と鑑別診断を中心に（心交感神経シンチグラフィを含む）．*INNERVISION*, **26**：21-24 (2011).
21) Weiner MW, Veitch DP, Aisen PS, Beckett LA, et al.: The Alzheimer's Disease Neuroimaging Initiative ; A review of papers published since its inception. *Alzheimers Dement*, **8** (1 Suppl.) : S1-68 (2012).
22) Yuan Y, Gu ZX, Wei WS : Fluorodeoxyglucose-positron-emission tomography, single-photon emission tomography, and structural MR imaging for prediction of rapid conversion to Alzheimer disease in patients with mild cognitive impairment ; A meta-analysis. *AJNR Am J Neuroradiol*, **30** : 404-410 (2009).
23) Zhang S, Han D, Tan X, Feng J, et al.: Diagnostic accuracy of [F-18]FDG and [C-11]PiB PET for prediction of short-term conversion to Alzheimer's disease in subjects with mild cognitive impairment. *Int J Clin Pract*, **66** : 185-198 (2012).

老年精神医学雑誌　第24巻第2号(2013. 2)別刷

特　集

アルツハイマー病診断のバイオマーカー；最近の進歩

形態 MRI，脳血流 SPECT および糖代謝 FDG-PET

伊藤健吾・加藤隆司